ACS SENSORS

pubs.acs.org/acssensors

Article

Fluorometric Viral miRNA Nanosensor for Diagnosis of Productive (Lytic) Human Cytomegalovirus Infection in Living Cells

Ji-Seon Lee, Seongchan Kim, Sungchul Kim, Kwangseog Ahn, and Dal-Hee Min*

Cite This: *ACS Sens.* 2021, 6, 815−822

Read Online

ACCESS | Metrics & More | Article Recommendations | Supporting Information

ABSTRACT: A human cytomegalovirus (HCMV) causes a persistent asymptomatic infection in healthy individuals and possesses unexpected dangers to newborn babies, immunocompromised people, and organ transplant recipients because of stealth transmission. Thus, an early and accurate diagnosis of HCMV infection is crucial for prevention of unexpected transmission and progression of the severe diseases. The standard method of HCMV diagnosis depends on serology, antigen test, and polymerase chain reaction-based nucleic acid detection, which have advantages for each target molecule. However, the serological test for an antibody is an indirect method assuming the past virus infection, and antigen and viral nucleic acid testing demand laborious, complex multistep procedures for direct virus detection. Herein, we present an alternative simple and facile fluorometric biosensor composed of a graphene oxide nanocolloid and fluorescent peptide nucleic acid (PNA) probe to detect the HCMV infection by simply monitoring the virally encoded microRNA as a new biomarker of lytic virus infection. We verify the sensing of HCMV-derived microRNA accumulated within 72 h after HCMV infection and examine the diagnosis of HCMV in living cells. We proceed with the time course and concentration-dependent investigation of hcmv-miRNA sensing in living cells as a direct method of HCMV detection at the molecular level on the basis of an intracellular hcmv-miRNA expression profile and graphene oxide nanocolloid-based simple diagnostic platform. The fluorometric biosensor enables the sequence-specific binding to the target HCMV miRNAs in HCMV-infected fibroblasts and shows the quantitative detection capability of HCMV infection to be as low as 4.15×10^5 immunofluorescence focus unit (IFU)/mL of the virus titer at 48 h post-infection with picomolar sensitivity for HCMV miRNA.

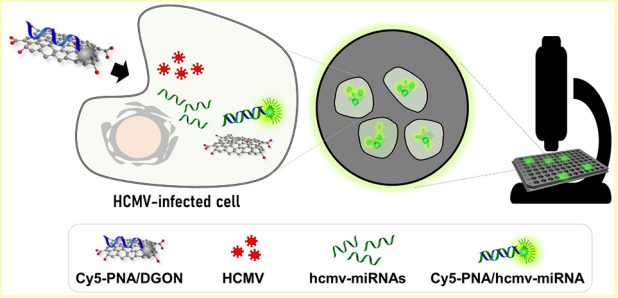

KEYWORDS: *asymptomatic infection, fluorometric biosensor, graphene oxide, HCMV infection, live-cell fluorescence imaging, viral microRNA*

An asymptomatic infectious disease possesses unexpected dangers such as Coronavirus disease 2019 (COVID-19) caused by SARS-CoV-2 because of stealth transmission.[1,2] One of the β-herpesviruses, the human cytomegalovirus (HCMV), cause a persistent asymptomatic infection to healthy individuals,[3−5] and most babies with congenital cytomegalovirus infection caused by intrauterine transmission during pregnancy are mostly asymptomatic. Nevertheless, it has become a leading cause of birth defects.[5,6] Moreover, opportunistic HCMV infection can induce infectious mortality in immunocompromised populations including newborns, human immunodeficiency virus (HIV)-infected people, or organ transplant recipients.[5,7,8] Thus, a simple and facile diagnosis of HCMV infection is crucial for preventing further viral spread and managing the progression of the severe diseases. The standard HCMV diagnosis relies on conventional methods including the serological test, antigen test, and polymerase chain reaction (PCR)-based nucleic acid detection.[9−12] The serological assays detect the past virus infection indirectly by measuring the host immune response to the virus such as the immunoglobulin G (IgG) or immunoglobulin M (IgM) antibody but cannot identify the virus itself directly.[12] In contrast, the antigen test and nucleic acid amplification test are direct methods targeting viral protein and viral genome, respectively. However, both methods are labor-intensive and require complex processes.[13] Therefore, we need an alternative strategy to address the shortcomings of the existing methods and to achieve a simple and facile detection of HCMV infection.

To date, microRNA (miRNA) has been suggested as a biomarker of disease diagnosis and prognosis in biomedical research fields.[14−18] Many studies have indicated that herpesviruses, a family of DNA virus, have their own viral miRNAs, which are virally encoded short non-coding RNAs

Received: September 3, 2020
Accepted: January 22, 2021
Published: February 2, 2021

containing ~22 nucleotides, and it has been revealed that HCMV encodes at least 22 kinds of its own viral miRNAs during the lytic phase of productive infection.[19−24] The hcmv-miRNAs have regulatory roles to the gene expression targeting both host cellular mRNA and viral RNA at the post-transcriptional level, and viral miRNAs offer valuable information of virus pathogenesis and play a crucial role in the virus life cycle, and interestingly, HCMV-derived miRNAs (hcmv-miRNAs) show an altered expression pattern after HCMV infection.[25,26] Thus, hcmv-miRNA sensing can be a direct channel for monitoring of the virus infection and pathogenesis at the molecular level.

In fact, a graphene-based fluorescent biosensor such as graphene oxide (GO) combined with a fluorescent oligo probe has been harnessed as a nucleic acid detection platform based on its advantages.[27−31] First, the π-conjugated electronic structure of GO induces the fluorescence quenching property at a close distance derived from its action as a FRET acceptor,[32] and GO has a preferential adsorption interaction with a single-stranded oligonucleotide over a double-stranded oligonucleotide originating from the $\pi-\pi$ stacking interaction,[28] which increases the utilization of GO as a sensor to discern the single-stranded nucleic acid from the double-stranded one. Also, the peptide nucleic acid (PNA), which has a neutral *N*-(2-aminoethyl)glycine backbone, gives distinctive features as a biosensor probe.[33] Regarding its adaptability for the living systems, the stability of the PNA probe in a biological environment derived from its structural unit of non-degradable DNA mimic and the resistance of the PNA probe to the nuclease and protease enzyme enable its application to living cells, which have complicated protein complexes.[33−36] Higher affinities between uncharged PNA and negatively charged GO can form stable PNA and a nanosized GO (NGO) complex, called PANGO in the previous report,[34] which can alleviate the electrostatic repulsion between a negatively charged phosphate backbone of the DNA probe and GO. Moreover, background fluorescence signals derived from nonspecific displacement of the fluorescent oligo probe from the GO surface can be minimized by using the PNA probe. Importantly, the target-binding affinity of uncharged PNA to its complementary target DNA or RNA strand is stronger than that of DNA to DNA or DNA to RNA, which can contribute the enhanced specificity of nucleic acid detection.[33−37] In addition, the miRNA-responsive PANGO system acting in sequence-specific manners *in vivo* was reported in a previous study[38] in which a dextran-coated partially reduced graphene oxide nanocolloid was utilized and particularly showed an improved stability and dispersibility of GO derivative via introduction of dextran, hydrophilic natural carbohydrate GO as a reducing agent, and a coating material of GO.[38,39] Herein, we developed a fluorometric HCMV miRNA sensor consisting of a dextran-coated graphene oxide nanocolloid (DGON) and fluorescent PNA probe for diagnosis and monitoring of HCMV infection in living cells. In this study, we utilized the virus-encoded miRNAs as a hallmark of virus infection and addressed hcmv-miRNAs as the diagnostic biomarker of productive HCMV infection (Figure 1). The aim of this study is to detect the viral miRNAs and visualize their expressions in living cells though fluorescence imaging for direct label-free detection of HCMV infection with a fluorometric sensor by targeting the viral miRNA without pre-enrichment. The fluorescent PNA and DGON-based biosensor can be alternative strategies of virus diagnosis to cope with the drawbacks of the conventional methods demanding laborious, complex multistep procedures.

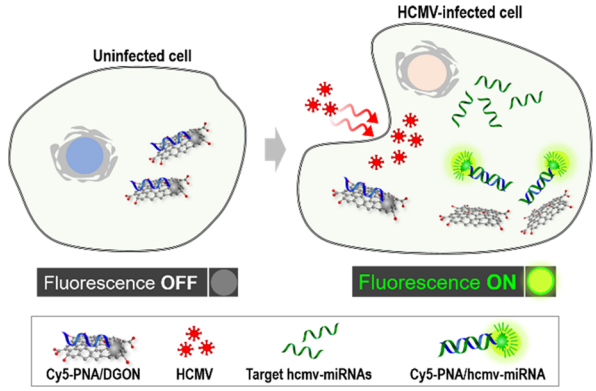

Figure 1. Schematic description of the HCMV diagnostic strategy, which is based on HCMV-encoded miRNA sensing in the HCMV-infected living cell by using Cy5-labeled PNA and the DGON system.

RESULTS AND DISCUSSIONS

Selection of Target HCMV miRNAs and Preparation of hcmv-miRNA Sensor System. To investigate the sensing of the intracellular HCMV-encoded miRNAs in HCMV-infected living cells, the miRNAs were divided into two experimental groups and two control groups. We chose hcmv-miR-US25-1-5p and hcmv-miR-UL112-3p as experimental groups, which have abundant expression levels after HCMV infection with distinctively increased expression profiles in the course of the HCMV infection time. In addition, hcmv-miR-US25-2-5p was chosen as a negative control group, which has a relatively lower expression level in the HCMV-infected cells compared to those of experimental groups. As a positive control group, hsa-miR-16-5p was utilized due to its high expression level in both HCMV-infected and uninfected cells. The expression profile of the target hcmv-miRNA candidates and hsa-miR-16 obtained in Table S1 is based on AGO-Clipseq analysis of the previous research.[25]

Next, we prepared the hcmv-miRNA sensors consisting of fluorescent dye-labeled PNA probes and DGON. Cyanine dye 5 (Cy5)-labeled single-stranded PNA probes (Cy5-PNA1, Cy5-PNA2, Cy5-PNA3, and Cy5-PNA16) were designed first, which have complementary sequences to the target miRNAs, including hcmv-miR-US25-1-5p, hcmv-miR-UL112-3p, hcmv-miR-US25-2-5p, and hsa-miR-16, respectively. As a negative control probe, a scrambled PNA (scPNA) was additionally prepared, which is not relevant to the target HCMV-encoded miRNAs (Figure 2A). Also, DGON was prepared according to the previously reported method[38,40] (see the Supporting Information). Synthesized DGON was characterized by using atomic force microscopy (AFM) with height profile, dynamic light scattering (DLS) and zeta potential analysis, and UV−vis absorption, Raman, and Fourier transform infrared (FT-IR) spectroscopies (Figure S1). The AFM data showed that the layer thickness of DGON was about 3.85 nm in average, which is greater than that of a single-layer graphene oxide nanocolloid (1−1.5 nm),[40] indicating the attachment of dextran on the graphene oxide nanocolloid.[38,41] The average zeta potential was −33.6 ± 0.6 mV, and the hydrodynamic diameter measured by DLS was 49.4 ± 17.6 nm. UV−vis absorption spectra indicated a maximum absorption at 238 nm resulting from the $\pi-\pi^*$ transition of aromatic C=C bonds. Raman

https://dx.doi.org/10.1021/acssensors.0c01843
ACS Sens. 2021, 6, 815−822

A

HCMV miRNA	Sequence (5' - 3')	[Flu]-PNA	Sequence (N term – C term)
hcmv-miR-US25-1-5p	AACCGCUCAGUGGCUCGGACC	Cy5-PNA1	Cy5-OO-GGTCCGAGCCACTGAGCG
hcmv-miR-UL112-3p	AAGUGACGGUGAGAUCCAGGCU	Cy5-PNA2	Cy5-OO-AGCCTGGATCTCACCGTC
hcmv-miR-US25-2-5p	AGCGGUCUGUUCAGGUGGAUGA	Cy5-PNA3	Cy5-OO-CCACCTGAACAGACCGCT
hsa-miR-16-5p	UAGCAGCACGUAAAUAUUGGCG	Cy5-PNA16	Cy5-OO-CGCCAATATTTACGTGCTGCTA
-	-	Cy5-scPNA	Cy5-OO-ATCGAATAGTCTGACTACAACT

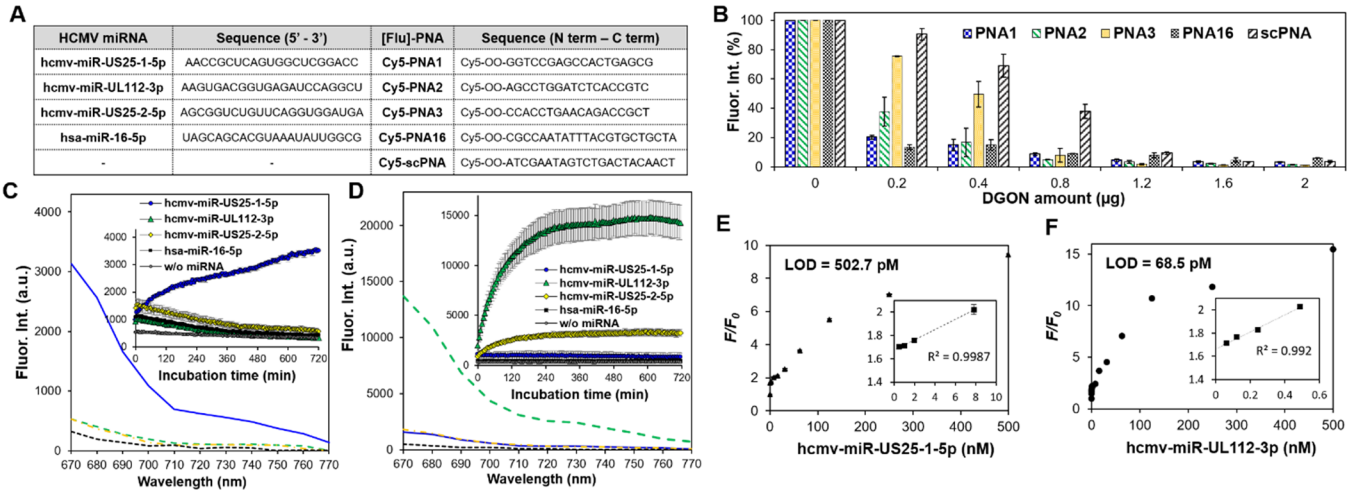

Figure 2. (A) Sequences of target hcmv-miRNAs, hsa-miR-16, and their corresponding Cy5-PNA probes designed in this study. (B) Relative fluorescence intensity (%) of each Cy5-PNA probe (20 pmol) was analyzed with increasing amounts of DGON. (Each of the fluorescence spectra is shown in Figure S2). (C) Fluorescence spectra of Cy5-PNA1/DGON (inset: the kinetics of the fluorescence recovery until 12 h) in the presence of hcmv-miR-US25-1-5p, hcmv-miR-UL112-3p, hcmv-US25-2-5p, and hsa-miR-16-5p. (D) Fluorescence spectra of Cy5-PNA2/DGON (inset: the kinetics of the fluorescence recovery until 12 h) in the presence of hcmv-miR-US25-1-5p, hcmv-miR-UL112-3p, hcmv-US25-2-5p, and hsa-miR-16-5p. (E) Relative fluorescence intensity (F/F_0) of Cy5-PNA1/DGON with serially diluted target hcmv-miR-US25-1-5p and (F) relative fluorescence intensity (F/F_0) of Cy5-PNA2/DGON with serially diluted target hcmv-miR-UL112-3p. (F, fluorescence intensity of the Cy5-PNA probe with target hcmv-miRNA; F_0, fluorescence intensity of the Cy5-PNA probe without target hcmv-miRNA). The excitation/emission wavelengths (λ_{ex}/λ_{em}) of the fluorescence intensity and spectra were 647/670 nm, respectively. The values are mean ± SEM (standard error of the mean), n = 3.

spectra showed the D and G peak at 1351 and 1592 cm^{-1}, which indicated the structural disorder sp^3 and ordered sp^2 carbon domain, respectively, and the D/G peak intensity ratio (I_D/I_G) was 0.91. FT-IR spectra exhibited the characteristic peaks of an O−H vibration at 3421.1 cm^{-1}, a weak aliphatic C−H stretching peak at 2920 cm^{-1}, a C═O stretching at 1716.3 cm^{-1}, and C═C vibrations of the graphitic domain at 1614 cm^{-1} and the several functional groups including the hydroxyl and carboxyl group. Taken together, these characterization data supported the successful preparation of DGON.

Feasibility Test of hcmv-miRNA Sensor System *In Vitro*. Before the analysis of the Cy5-PNA/DGON system, hybridization interactions between the Cy5-PNAs and the target miRNAs were demonstrated through non-denaturing polyacrylamide gel electrophoresis (Figure S2). The upper bands represented each of the three Cy5-PNAs (Cy5-PNA1, Cy5-PNA2, and Cy5-PNA3) visualized as red fluorescence, and lower bands shown as green colors were target hcmv-miRNAs for each Cy5-PNA. The PNA/miRNA duplexes appeared in the middle as the red colors, which showed the migration of the PNA bands due to the hybridization to the target hcmv-miRNAs. To construct the viral miRNA sensor system composed of the Cy5-PNA probe and DGON, the ratio of PNA to DGON was discovered by measuring the fluorescence intensity of each Cy5-PNA probe with the increasing amount of DGON. By simply mixing the Cy5-PNA probe with DGON as a homogeneous mixture in phosphate-buffered saline (1× PBS) conditions, a fluorescent dye-labeled single-stranded PNA probe could be easily adsorbed on the surface of DGON. As a result, the fluorescence of Cy5-PNA (20 pmol) was quenched down to 5% of initial intensity, indicating the strong interaction between Cy5-PNA and DGON. Ratios of of DGON per 10 pmol of Cy5-PNA were determined to be 0.6 μg for PNA1 and PNA3, 0.4 μg for PNA2, and 0.8 μg for PNA16 and scPNA, and these optimal ratios were maintained for further experiments in this study (Figure 2B and Figure S3).

We next investigate the feasibility of the hcmv-miRNA sensor *in vitro*. To evaluate the specificity of the hcmv-miRNA sensors, the fluorescence of Cy5-PNAs/DGON was measured in the presence of the target hcmv-miRNAs (see the Experimental Section). As shown in Figure 2C and Figure 2D, the quenched fluorescence of each Cy5-PNA1 and PNA2 probe was recovered only in the existence of its corresponding target hcmv-miR-US25-1-5p and hcmv-miR-UL112-3p, respectively; however, it remains quenched with non-target miRNAs. In the case of the other two control PNA groups of Cy5-PNA3/DGON and Cy5-PNA16/DGON, their specificities for hcmv-miR-US25-2-5p and hsa-miR-16 were tested individually (Figure S4) in the same manner as the two experimental groups of Cy5-PNA1/DGON and Cy5-PNA2/DGON, as mentioned above. Consequently, sequence-specific recognition of the designed PNA probes in complex with DGON (Cy5-PNA/DGON) to the target hcmv-miRNAs was successfully demonstrated *in vitro*.

Also, the sensitivity of the hcmv-miRNA sensors was examined *in vitro* (see the Experimental Section). In the case of the hcmv-miR-US25-1-5p sensor (Cy5-PNA1/DGON), it shows the linearity in a range of 488.3−7812.5 pM with a detection limit of 502.7 pM (Figure 2E), and the hcmv-miR-UL112-3p sensor (Cy5-PNA2/DGON) shows the linearity in a range of 61.0−488.3 pM with a detection limit of 68.5 pM (Figure 2F). These results are comparable to the previously reported behavior of the PNA/GO-based sensor system.[42,43]

Sensing of hcmv-miRNAs for Diagnosis of HCMV Infection in Living Cells. To demonstrate the diagnosis of HCMV infection in living cells, we used primary human foreskin fibroblast (HFF), generally known for being permissive to HCMV infection,[9,44] and examined the cytotoxicity of DGON (0−450 μg/mL), three Cy5-PNA probes, and the Cy5-PNA/DGON systems after treatment for

https://dx.doi.org/10.1021/acssensors.0c01843
ACS Sens. 2021, 6, 815−822

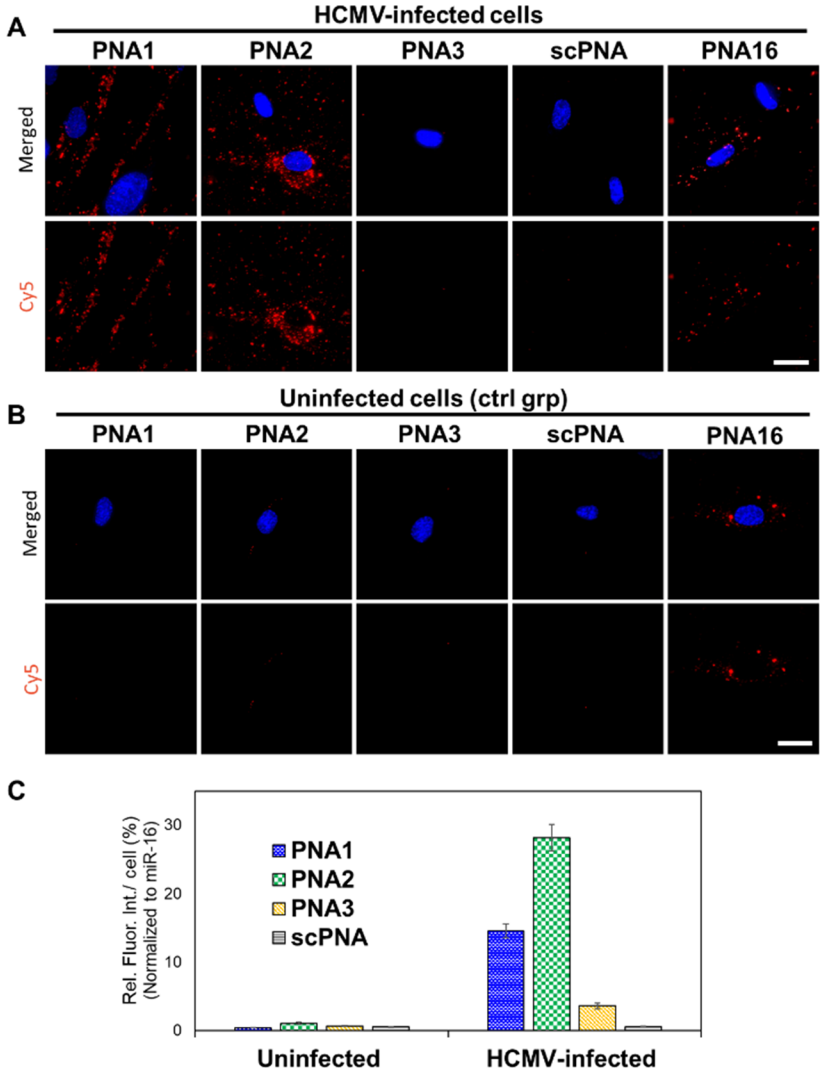

Figure 3. Fluorescence images of the (A) HCMV-infected group (72 h) and (B) uninfected control group (ctrl grp) in HFF cells after treatment of each hcmv-miRNA sensor (Cy5-PNA/DGON: PNA1, PNA2, PNA3, scPNA, or PNA16 with each optimal amount of DGON) for 12 h. The fluorescence images were obtained with living cells. Scale bars are 25 μm. (C) Quantitative analysis of intracellular fluorescence signals of each HCMV miRNA sensor in living cells was performed for HCMV-infected (72 h) and uninfected (ctrl grp) HFF cells, and data shown in the graph are normalized to the value of hsa-miR-16 as mean ± SEM (standard error of the mean), n = 3.

12 h. As a result, DGON represented ~99% of cell viability in a range of 0−14.1 μg/mL (10.7 ± 2.3 μg/mL of DGON was applied to the HFFs for further studies). Also, Cy5-PNA probes (Cy5-PNA1, Cy5-PNA2, and Cy5-PNA3) and each Cy5-PNA/DGON complex (Cy5-PNA1/DGON, Cy5-PNA2/DGON, and Cy5-PNA3/DGON) did not show any cytotoxicity and represent ~100% of the cell viability. (Figure S5). For HCMV infection, HCMV $Towne_{long}$ strain (5.62×10^6 IFU/mL, where IFU stands for the immunofluorescence focus unit; Figure S6) was inoculated to the HFF cells at 9.37 MOI (multiplicity of infection) and the cells were incubated until 72 h. Then, we applied each hcmv-miRNA sensor system composed of Cy5-PNA/DGON to HCMV-infected and uninfected HFF cells. The resulting fluorescence signals were analyzed by fluorescence imaging, and each of their quantities was normalized by the signals for positive control, hsa-miR-16. As shown in Figure 3 and Figure S8, Cy5-PNA1/DGON-treated HCMV-infected cells exhibited a 36-fold higher fluorescence intensity compared to uninfected cells, while Cy5-PNA2/DGON-treated infected cells showed a 27-fold stronger fluorescence signal than that of uninfected cells. In contrast, the Cy5-PNA3/DGON-treated control group exhibited 5.5-fold differences of fluorescence signals between HCMV-infected and uninfected cells, which reflected a relatively lower expression level of its target hcmv-miR-US25-2-5p compared to that of hcmv-miR-US25-1-5p or hcmv-miR-UL112-3p in HCMV-infected cells. The negative control group of the Cy5-scPNA/DGON-treated HCMV-infected and uninfected cells did not show any detectable fluorescence signals. In particular, the fluorescence signals derived from individual Cy5-PNA1/DGON-, Cy5-PNA2/DGON-, and Cy5-PNA3/DGON-treated cases in HCMV-infected cells exhibited 25.3, 48.9, and 6.3 times higher values compared to that of Cy5-scPNA/DGON-treated HCMV-infected cells, respectively, indicating the sequence-specific detection capability of hcmv-miRNA sensors to each of their target miRNAs. As the positive control, Cy5-PNA16/DGON-treated HFF cells clearly showed red fluorescence signals corresponding to hsa-miR-16 in the cytoplasm of both HCMV-infected and uninfected HFF cells. Collectively, it is

https://dx.doi.org/10.1021/acssensors.0c01843
ACS Sens. 2021, 6, 815−822

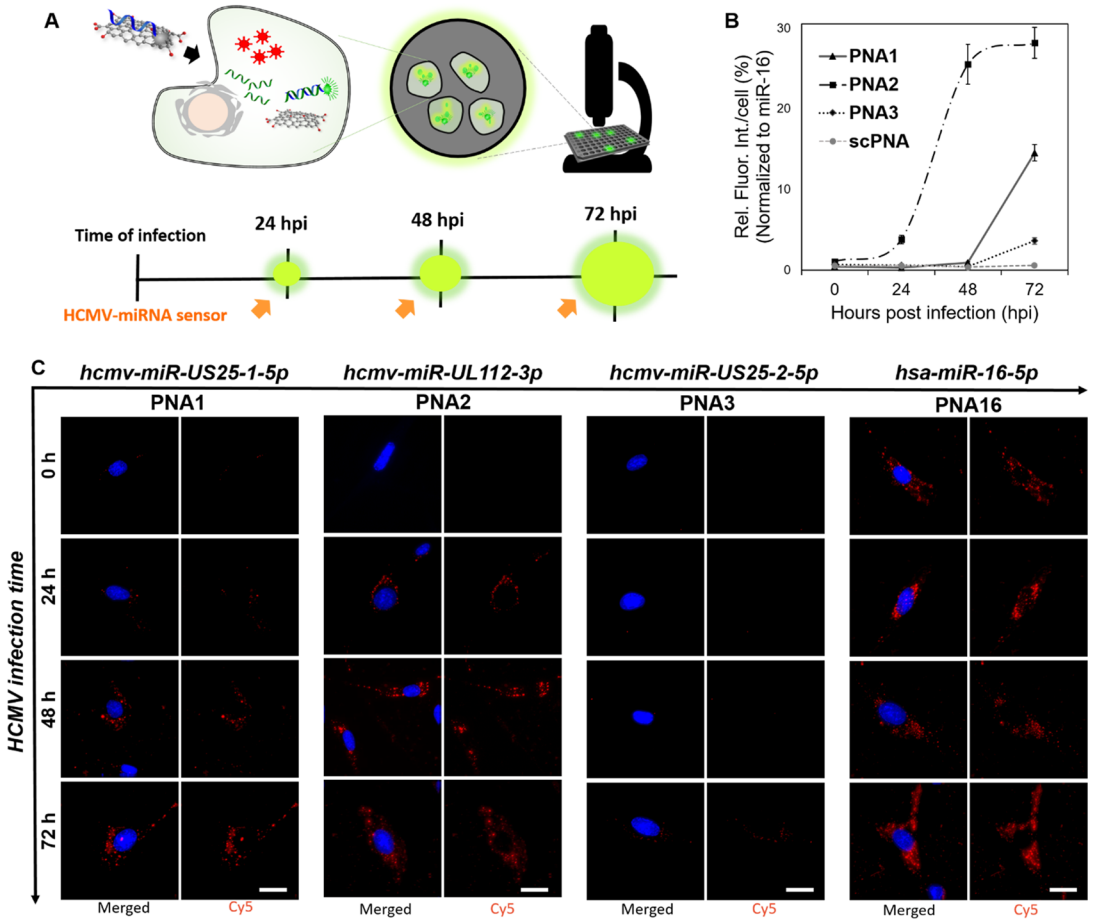

Figure 4. (A) Schematic illustration of the HCMV diagnostic process in terms of the time of virus infection. (B) Quantitative analysis of intracellular fluorescence signals of each HCMV miRNA sensor system (Cy5-PNA1/DGON, Cy5-PNA2/DGON, and Cy5-PNA3/DGON) and Cy5-scPNA/DGON in living cells according to the time of virus infection (0, 24, 48, and 72 h). The data shown in the graph are normalized relative to the value of hsa-miR-16 (Cy5-PNA16/DGON) as mean ± SEM (standard error of the mean), n = 3. (C) Fluorescence images of each HCMV miRNA sensor system (Cy5-PNA1/DGON, Cy5-PNA2/DGON, and Cy5-PNA3/DGON) and Cy5-PNA16/DGON after the time course of HCMV infection (0, 24, 48, and 72 h) in HFF cells. Each 20 pmol of PNA was treated for 12 h with an optimal amount of DGON. The scale bars are 25 μm (in the case of Cy5-scPNA/DGON, the negative ctrl grp and the fluorescence images were added, as shown in the Supporting Information, Figure S9D).

demonstrated that the HCMV-infected and uninfected cells represented significantly different intracellular fluorescence signals for hcmv-miR-US25-1-5p, hcmv-miR-UL112-3p, and hcmv-miR-US25-2-5p, and the hcmv-miRNA sensors composed of Cy5-PNA and DGON could distinguish the HCMV infection from uninfected cases and recognize the target viral miRNA in a sequence-specific manner at the same time.

Sensing of hcmv-miRNAs in Living Cells According to the Time of HCMV Infection and Virus Titer. We next investigate the time course measurement of hcmv-miRNA signals in HCMV-infected living cells with respect to the four different stages of uninfected (0 h) and infected (24, 48, and 72 h) conditions to monitor the different stages of HCMV infection (Figure 4A and Figure S7, Supporting Information). As shown in Figure 4B,C and Figures S9 and S10, the Cy5-PNA2/DGON-treated group clearly exhibited the red fluorescence signals after HCMV infection with an increased tendency of the fluorescence intensity according to the time of HCMV infection, possibly driven by the increased hcmv-miR-UL112-3p expression with the HCMV infection time. However, the groups treated with Cy5-PNA1/DGON and Cy5-PNA3/DGON did not obviously exhibit the tendency of fluorescence increases in the time of infection (0−48 h) in contrast with the fluorescence signals that distinctively shown the differences between the 72 h infected and uninfected (0 h) cells. Based on these results, we noticed that the performance of the Cy5-PNA2/DGON system for hcmv-miR-UL112-3p was relatively sophisticated for discerning the different infection stages of HCMV and hcmv-miRNA expression levels. To further assess the quantification potential of HCMV in living cells, we tested the Cy5-PNA2/DGON system in HCMV-infected HFF cells at 48 h post-infection with a different initial virus titer (Figure 5). After treating the Cy5-PNA2/DGON system, the fluorescence images and quantities were analyzed. As shown in Figure 5C, the calibration curve for the virus titer lower than 1.87 (10^6 IFU/mL) showed a linear correlation (R^2 = 0.9803) between the virus titer and relative fluorescence intensity per cell, and the LOD was estimated to be as low as 4.15 × 10^5 IFU/mL, which is consistent with the previously reported cell-based fluorescent biosensors.[45−47] Altogether, we verified the performance of the hcmv-miRNA sensor system for its capability of distinguishing the virus-infected degrees in terms of the time of HCMV infection and the virus titer. Particularly, the Cy5-PNA2/DGON system for

https://dx.doi.org/10.1021/acssensors.0c01843
ACS Sens. 2021, 6, 815−822

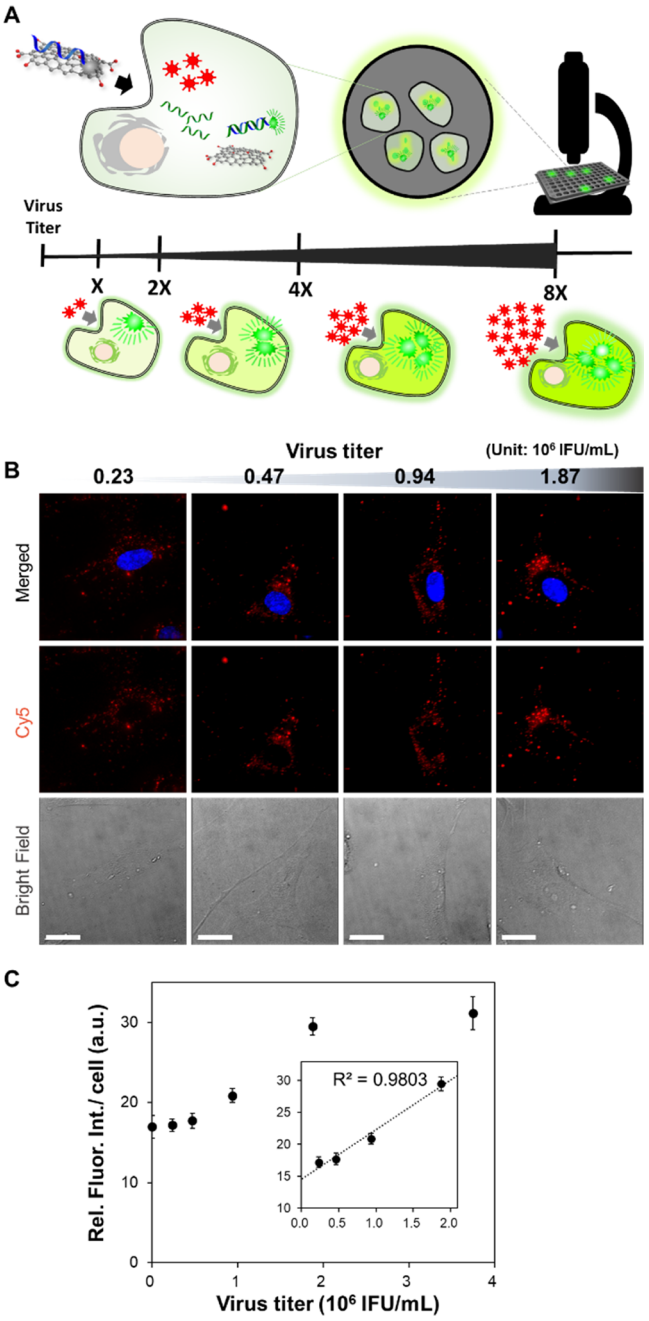

Figure 5. (A) Schematic illustration of the HCMV diagnostic process in terms of the initial virus titer. (B) Initial HCMV concentration-dependent fluorescence signals of the HCMV miRNA sensor system (Cy5-PNA2/DGON) in HCMV-infected HFF cells (48 h). The fluorescence images were obtained in living cells. The scale bars are 25 μm. (C) Relative fluorescence intensity per cell (a.u.) was analyzed. Data shown in the graph are the value of mean ± SEM, n = 3.

hcmv-miR-UL112-3p could track the changes of its expression under 24, 48, and 72 h infected conditions in detail, and the fluorescence signals from the Cy5-PNA2/DGON system represented the positive correlation with the initial HCMV titer, and thus, these results demonstrate the quantitative sensing of HCMV, suggesting the potential of this hcmv-miRNA sensor for accurate HCMV diagnosis.

CONCLUSIONS

Early and accurate diagnosis of the virus infection is a major concern against the virus spread. Of note, hcmv-miRNA can be an alternative biomarker for facile early detection within 72 h and for accurate detection of the live virus. In the present study, we selected the three different hcmv-miRNAs, hcmv-miR-US25-1-5p, hcmv-miR-UL112-3p, and hcmv-miR-US25-2-5p, and explored the role of the HCMV miRNAs as the biomarker and addressed the potential of the virus diagnostic indicator to cope with the asymptomatic stealth HCMV infection. We demonstrated the Cy5-PNA/DGON-based fluorometric virus diagnostic sensor to monitor the HCMV infection up to 72 h easily by detecting the virally encoded miRNA produced during lytic HCMV infection in living cells. The Cy5-PNA/DGON-based HCMV miRNA sensors could diagnose HCMV infection from uninfected cells with a sequence-specific response to the target viral miRNAs and could discern the changes of hcmv-miRNA expression according to the infection time and the initial virus titer.

Currently, the danger of the asymptomatic virus transmission has been experienced since the COVID-19 outbreaks. Primary HCMV infection is typically asymptomatic, and it is hard to detect the virus before the onset of clinical symptoms because viral samples may not contain enough viral components required for the detection in this incubation period. In this respect, targeting hcmv-miRNA, which is abundantly accumulated within 72 h after HCMV infection, can be an alternative method for presymptomatic diagnosis of HCMV. Also, false-positive results in the diagnostic test that originated from the dead virus fragments exhibiting a loss in infectivity can be alleviated by detecting the hcmv-miRNAs produced by a live virus with the PNA/DGON-based simple diagnostic system.

Furthermore, we suggest that this HCMV miRNA-responsive sensor system can be further applied to establishing a cell-based high-content screening platform for antiviral drug discovery exploiting currently known HCMV miRNAs as the novel therapeutic targets of lytic HCNV infection.

EXPERIMENTAL SECTION

Optimization of the Cy5-PNA/DGON System *In Vitro*. To determine the optimal amount of DGON corresponding to each Cy5-PNA probe, the fluorescence quenching test was performed in 1× PBS solution. The fluorescence of each Cy5-PNA probe (20 pmol) was measured after addition of an increasing amount of DGON (0−2 μg) by using a fluorometer SynergyMx (Biotek, UK). The total volume of each sample solution was 50 μL. To evaluate the specificity of hcmv-miRNA sensors, the synthetic hcmv-miRNAs (20 pmol) including hcmv-miR-US25-1-5p, hcmv-miR-UL112-3p, hcmv-miR-US25-2-5p, and hsa-miR-16 were added to each Cy5-PNA probe (20 pmol) and DGON mixture (total volume 100 μL, 1× PBS conditions), and the fluorescence was measured at 5 min intervals (0−720 min). To examine the detection sensitivity of hcmv-miRNA sensors, serially diluted synthetic single-stranded hcmv-miR-US25-1-5p and hcmv-miR-UL112-3p (0−500 nM) were added to each mixture of the Cy5-PNA1 or Cy5-PNA2 probe (500 nM) with an optimized amount of DGON (total 100 μL) followed by measuring fluorescence intensities. The LOD was estimated according to the formula LOD = 3.3 (SD/S) (SD, standard deviation of the regression line; S, slope of the calibration curve).[48]

Viral miRNA Sensing in HCMV-Infected Living Cells with Fluorescence Imaging Tool. HFF cells were seeded to an 8-well glass chamber slide and a 96-well culture plate with a density of 2.0 × 10^4 cells per well for 24 h. HCMV was inoculated at 9.37 MOI corresponding to 0.94 × 10^6 IFU/mL, and the cells were harvested at

https://dx.doi.org/10.1021/acssensors.0c01843
ACS Sens. 2021, 6, 815−822

a designated post-infection time. As for the four different initial virus titers, 2-fold serially diluted HCMV stocks from 1.87×10^6 to 0.23×10^6 IFU/mL were inoculated in HFF cells and the cells were harvested for 48 h. Then, the cells were treated with each Cy5-PNA/DGON for 12 h in a serum-free medium to a final volume of 100 μL. After the cells were briefly rinsed with 1× PBS, the media were replaced with a serum-containing complete medium. Fluorescence images were obtained by using a DeltaVision Elite microscopy system (GE Healthcare, USA) and IN Cell Analyzer 2000 (GE Healthcare, USA). For quantitative analysis of the intracellular fluorescence signals in living cells, the fluorescence images were analyzed with an IN Cell Analyzer 1000 Developer Toolbox and Analysis Workstation software.

Other materials and methods used in this study are described in the Supporting Information.

■ ASSOCIATED CONTENT

Supporting Information

The Supporting Information is available free of charge at https://pubs.acs.org/doi/10.1021/acssensors.0c01843.

Experimental section (preparation and characterization of DGON, cell culture, cell viability assay with DGON, titration of HCMV, and RT-qPCR); AGO-Clipseq analysis of the hcmv-miRNA expression profile; characterization data of DGON; fluorescence spectral analysis of Cy5-PNA/DGON; the cell viability assay with PNA, DGON, and PNA/DGON; titration of HCMV; RT-qPCR analysis for HCMV lytic replication and production; and fluorescence images related to Figures 3 and 4C (PDF)

■ AUTHOR INFORMATION

Corresponding Author

Dal-Hee Min − *Department of Chemistry and School of Biological Sciences, Seoul National University, Seoul 08826, Republic of Korea; Institute of Biotherapeutics Convergence Technology, Lemonex Inc., Seoul 08826, Republic of Korea;* orcid.org/0000-0001-8623-6716; Email: dalheemin@snu.ac.kr

Authors

Ji-Seon Lee − *Department of Chemistry, Seoul National University, Seoul 08826, Republic of Korea;* orcid.org/0000-0003-2221-2859

Seongchan Kim − *Department of Chemistry, Seoul National University, Seoul 08826, Republic of Korea;* orcid.org/0000-0002-2104-6599

Sungchul Kim − *Center for RNA Research, Institute for Basic Science (IBS), Seoul 08826, Republic of Korea; School of Biological Sciences, Seoul National University, Seoul 08826, Republic of Korea*

Kwangseog Ahn − *Center for RNA Research, Institute for Basic Science (IBS), Seoul 08826, Republic of Korea; School of Biological Sciences, Seoul National University, Seoul 08826, Republic of Korea*

Complete contact information is available at: https://pubs.acs.org/10.1021/acssensors.0c01843

Author Contributions

J.-S.L. designed and performed the synthesis and characterization of DGON, *in vitro* test, and live-cell fluorescence imaging with data analysis and wrote the paper. Seongchan Kim performed the immunofluorescence assay and live-cell fluorescence imaging and gave the advice for AFM analysis of DGON. Sungchul Kim gave the intellectual advice for HCMV miRNAs and provided the HCMV $Towne_{long}$ strain and HFFs. K.A. supported the knowledge of HCMV virology. D.-H.M. designed and performed the overall data analysis and intellectual interpretations and wrote the paper.

Notes

The authors declare the following competing financial interest(s): D.-H. Min is named on patents about the fluorescent sensors based on carbon nanomaterials. D.-H. Min is a co-founder of Lemonex Inc. The remaining authors declare no competing interests.

■ ACKNOWLEDGMENTS

This work was supported by Lemonex Inc. (LEMONEX-SN201709-3-12 and LEMONEX-SN201901-3-30) and the Basic Science Research Program (2016R1E1A1A01941202 and 2016R1A4A1010796) through the National Research Foundation of Korea (NRF).

■ REFERENCES

(1) Rothe, C.; Schunk, M.; Sothmann, P.; Bretzel, G.; Froeschl, G.; Wallrauch, C.; Zimmer, T.; Thiel, V.; Janke, C.; Guggemos, W.; Seilmaier, M.; Drosten, C.; Vollmar, P.; Zwirglmaier, K.; Zange, S.; Wölfel, R.; Hoelscher, M. Transmission of 2019-nCoV Infection From an Asymptomatic Contact in Germany. *N. Engl. J. Med.* **2020**, *382*, 970−971.

(2) Li, R.; Pei, S.; Chen, B.; Song, Y.; Zhang, T.; Yang, W.; Shaman, J. Substantial undocumented infection facilitates the rapid dissemination of novel coronavirus (SARS-CoV-2). *Science* **2020**, *368*, 489−493.

(3) Zanghellini, F.; Boppana, S. B.; Emery, V. C.; Griffiths, P. D.; Pass, R. F. Asymptomatic Primary Cytomegalovirus Infection: Virologic and Immunologic Features. *J. Infect. Dis.* **1999**, *180*, 702−707.

(4) Mocarski, E. S.; Courcelle, C. T. Cytomegaloviruses and their replication. *Fields Virology* **2001**, 2629−2673.

(5) Crough, T.; Khanna, R. Immunobiology of human cytomegalovirus: from bench to bedside. *Clin. Microbiol. Rev.* **2009**, *22*, 76−98.

(6) Boppana, S. B.; Ross, S. A.; Fowler, K. B. Congenital cytomegalovirus infection: clinical outcome. *Clin. Infect. Dis.* **2013**, *57*, S178−S181.

(7) Savva, G. M.; Pachnio, A.; Kaul, B.; Morgan, K.; Huppert, F. A.; Brayne, C.; Moss, P. A. H. Cytomegalovirus Infection Is Associated with Increased Mortality in the Older Population. *Aging Cell* **2013**, *12*, 381−387.

(8) Sia, I. G.; Patel, R. New strategies for prevention and therapy of cytomegalovirus infection and disease in solid-organ transplant recipients. *Clin. Microbiol. Rev.* **2000**, *13*, 83−121.

(9) Revello, M. G.; Gerna, G. Diagnosis and management of human cytomegalovirus infection in the mother, fetus, and newborn infant. *Clin. Microbiol. Rev.* **2002**, *15*, 680−715.

(10) Ross, S. A.; Novak, Z.; Pati, S.; Boppana, S. B. Overview of the Diagnosis of Cytomegalovirus Infection. *Infect. Disord. Drug. Targets.* **2011**, *11*, 466−474.

(11) Drew, W. L. Laboratory diagnosis of cytomegalovirus infection and disease in immunocompromised patients. *Curr. Opin. Infect. Dis.* **2007**, *20*, 408−411.

(12) Lazzarotto, T.; Guerra, B.; Lanari, M.; Gabrielli, L.; Landini, M. P. New advances in the diagnosis of congenital cytomegalovirus infection. *J. Clin. Virol.* **2008**, *41*, 192−197.

(13) Schäfer, P.; Tenschert, W.; Gutensohn, K.; Laufs, R. Minimal effect of delayed sample processing on results of quantitative PCR for cytomegalovirus DNA in leukocytes compared to results of an antigenemia assay. *J. Clin. Microbiol.* **1997**, *35*, 741−744.

(14) Hayes, J.; Peruzzi, P. P.; Lawler, S. MicroRNAs in cancer: Biomarkers, functions and therapy. *Trends Mol. Med.* **2014**, *20*, 460−469.

(15) Wang, J.; Chen, J.; Sen, S. MicroRNA as Biomarkers and Diagnostics. *J. Cell. Physiol.* **2016**, *231*, 25−30.
(16) Chen, Z.; Liang, H.; Chen, X.; Ke, Y.; Zhou, Z.; Yang, M.; Zen, K.; Yang, R.; Liu, C.; Zhang, C.-Y. An Ebola virus-encoded microRNA-like fragment serves as a biomarker for early diagnosis of Ebola virus disease. *Cell Res.* **2016**, *26*, 380−383.
(17) Drury, R. E.; O'Connor, D.; Pollard, A. J. The Clinical Application of MicroRNAs in Infectious Disease. *Front. Immunol.* **2017**, *8*, 1182.
(18) Condrat, C. E.; Thompson, D. C.; Barbu, M. G.; Bugnar, O. L.; Boboc, A.; Cretoiu, D.; Suciu, N.; Cretoiu, S. M.; Voinea, S. C. miRNAs as Biomarkers in Disease: Latest Findings Regarding Their Role in Diagnosis and Prognosis. *Cell* **2020**, *9*, 276−307.
(19) Pfeffer, S.; Zavolan, M.; Grässer, F. A.; Chien, M.; Russo, J. J.; Ju, J.; John, B.; Enright, A. J.; Marks, D.; Sander, C.; Tuschl, T. Identification of virus-encoded microRNAs. *Science* **2004**, *304*, 734−736.
(20) Pfeffer, S.; Sewer, A.; Lagos-Quintana, M.; Sheridan, R.; Sander, C.; Grässer, F. A.; van Dyk, L. F.; Ho, C. K.; Shuman, S.; Chien, M.; Russo, J. J.; Ju, J.; Randall, G.; Lindenbach, B. D.; Rice, C. M.; Simon, V.; Ho, D. D.; Zavolan, M.; Tuschl, T. Identification of microRNAs of the herpesvirus family. *Nat. Methods* **2005**, *2*, 269−276.
(21) Dunn, W.; Trang, P.; Zhong, Q.; Yang, E.; van Belle, C.; Liu, F. Human cytomegalovirus expresses novel microRNAs during productive viral infection. *Cell. Microbiol.* **2005**, *7*, 1684−1695.
(22) Grey, F.; Antoniewicz, A.; Allen, E.; Saugstad, J.; McShea, A.; Carrington, J. C.; Nelson, J. Identification and characterization of human cytomegalovirus-encoded microRNAs. *J. Virol.* **2005**, *79*, 12095−12099.
(23) Hook, L.; Hancock, M.; Landais, I.; Grabski, R.; Britt, W.; Nelson, J. A. Cytomegalovirus microRNAs. *Curr. Opin. Virol.* **2014**, *7*, 40−46.
(24) Gottwein, E.; Cullen, B. R. Viral and cellular microRNAs as determinants of viral pathogenesis and immunity. *Cell Host Microbe* **2008**, *3*, 375−387.
(25) Kim, S.; Seo, D.; Kim, D.; Hong, Y.; Chang, H.; Baek, D.; Kim, V. N.; Lee, S.; Ahn, K. Temporal Landscape of MicroRNA-Mediated Host-Virus Crosstalk during Productive Human Cytomegalovirus Infection. *Cell Host Microbe* **2015**, *17*, 838−851.
(26) Louten, J.; Beach, M.; Palermino, K.; Weeks, M.; Holenstein, G. MicroRNAs Expressed during Viral Infection: Biomarker Potential and Therapeutic Considerations. *Biomark Insights* **2015**, *10*, 25−52.
(27) Lee, J.; Kim, J.; Kim, S.; Min, D. H. Biosensors based on graphene oxide and its biomedical application. *Adv Drug Deliver Rev* **2016**, *105*, 275−287.
(28) He, S.; Song, B.; Li, D.; Zhu, C.; Qi, W.; Wen, Y.; Wang, L.; Song, S.; Fang, H.; Fan, C. A Graphene Nanoprobe for Rapid, Sensitive, and Multicolor Fluorescent DNA Analysis. *Adv. Funct. Mater.* **2010**, *20*, 453−459.
(29) Lu, C. H.; Yang, H. H.; Zhu, C. L.; Chen, X.; Chen, G. N. A graphene platform for sensing biomolecules. *Angew. Chem., Int. Ed. Engl.* **2009**, *48*, 4785−4787.
(30) Chen, J.; Shi, C.; Kang, X. Y.; Shen, X. T.; Lao, X.; Zheng, H. Recent advances in fluorescence resonance energy transfer-based probes in nucleic acid diagnosis. *Anal. Methods* **2020**, *12*, 884−893.
(31) Dong, H.; Zhang, J.; Ju, H.; Lu, H.; Wang, S.; Jin, S.; Hao, K.; Du, H.; Zhang, X. Highly Sensitive Multiple microRNA Detection Based on Fluorescence Quenching of Graphene Oxide and Isothermal Strand-Displacement Polymerase Reaction. *Anal. Chem.* **2012**, *84*, 4587−4593.
(32) Swathi, R. S.; Sebastian, K. L. Resonance energy transfer from a dye molecule to graphene. *J Chem Phys* **2008**, *129*, No. 054703.
(33) Egholm, M.; Buchardt, O.; Nielsen, P. E.; Berg, R. H. Peptide Nucleic-Acids (Pna) - Oligonucleotide Analogs with an Achiral Peptide Backbone. *J. Am. Chem. Soc.* **1992**, *114*, 1895−1897.
(34) Ryoo, S. R.; Lee, J.; Yeo, J.; Na, H. K.; Kim, Y. K.; Jang, H.; Lee, J. H.; Han, S. W.; Lee, Y.; Kim, V. N.; Min, D. H. Quantitative and Multiplexed MicroRNA Sensing in Living Cells Based on Peptide Nucleic Acid and Nano Graphene Oxide (PANGO). *ACS Nano* **2013**, *7*, 5882−5891.
(35) Egholm, M.; Buchardt, O.; Christensen, L.; Behrens, C.; Freier, S. M.; Driver, D. A.; Berg, R. H.; Kim, S. K.; Norden, B.; Nielsen, P. E. PNA hybridizes to complementary oligonucleotides obeying the Watson-Crick hydrogen-bonding rules. *Nature* **1993**, *365*, 566−568.
(36) Nielsen, P.; Egholm, M.; Berg, R.; Buchardt, O. Sequence-selective recognition of DNA by strand displacement with a thymine-substituted polyamide. *Science* **1991**, *254*, 1497−1500.
(37) Kotikam, V.; Fernandes, M.; Kumar, V. A. Comparing the interactions of DNA, polyamide (PNA) and polycarbamate nucleic acid (PCNA) oligomers with graphene oxide (GO). *Phys. Chem. Chem. Phys.* **2012**, *14*, 15003−15006.
(38) Lee, J. S.; Kim, S.; Na, H. K.; Min, D. H. MicroRNA-Responsive Drug Release System for Selective Fluorescence Imaging and Photodynamic Therapy In Vivo. *Adv. Healthcare Mater.* **2016**, *5*, 2386−2395.
(39) Zhu, C.; Guo, S.; Fang, Y.; Dong, S. Reducing Sugar: New Functional Molecules for the Green Synthesis of Graphene Nanosheets. *ACS Nano* **2010**, *4*, 2429−2437.
(40) Luo, J.; Cote, L. J.; Tung, V. C.; Tan, A. T. L.; Goins, P. E.; Wu, J.; Huang, J. Graphene Oxide Nanocolloids. *J. Am. Chem. Soc.* **2010**, *132*, 17667−17669.
(41) Xu, M.; Zhu, J.; Wang, F.; Xiong, Y.; Wu, Y.; Wang, Q.; Weng, J.; Zhang, Z.; Chen, W.; Liu, S. Improved In Vitro and In Vivo Biocompatibility of Graphene Oxide through Surface Modification: Poly(Acrylic Acid)-Functionalization is Superior to PEGylation. *ACS Nano* **2016**, *10*, 3267−3281.
(42) Lee, J.; Park, G.; Min, D. H. A biosensor for the detection of single base mismatches in microRNA. *Chem. Commun.* **2015**, *51*, 14597−14600.
(43) Ahn, S. M.; Kang, S.; Min, D. H. Direct Monitoring of Cancer-Associated mRNAs in Living Cells to Evaluate the Therapeutic RNAi Efficiency Using Fluorescent Nanosensor. *Acs Sensors* **2019**, *4*, 1174−1179.
(44) Compton, T. An immortalized human fibroblast cell line is permissive for human cytomegalovirus infection. *J. Virol.* **1993**, *67*, 3644−3648.
(45) Guerreiro, M. R.; Freitas, D. F.; Alves, P. M.; Coroadinha, A. S. Detection and Quantification of Label-Free Infectious Adenovirus Using a Switch-On Cell-Based Fluorescent Biosensor. *Acs Sensors* **2019**, *4*, 1654−1661.
(46) Milrot, E.; Makdasi, E.; Politi, B.; Israely, T.; Laskar, O. A Cell-Based Capture Assay for Rapid Virus Detection. *Viruses* **2020**, *12*, 1165.
(47) Lambeth, C. R.; White, L. J.; Johnston, R. E.; de Silva, A. M. Flow cytometry-based assay for titrating dengue virus. *J. Clin. Microbiol.* **2005**, *43*, 3267−3272.
(48) J. C., Miller, J. N., Miller, *Statistics and Chemometrics for Analytical Chemistry*; 2005, 5th ed., Pearson Prentice hall: Edinburgh

https://dx.doi.org/10.1021/acssensors.0c01843
ACS Sens. 2021, 6, 815−822